

Near-Earth asteroid regolith properties from thermal mm-wavelength observations

T. N. Titus¹, A. Moullet², H. Hsieh³, N. Roth^{4,5} & X. D. Zou³

¹U.S. Geological Survey, 2255 N. Gemini Dr., Flagstaff, AZ 86001, USA (titus@usgs.gov),
²National Radio Astronomy Observatory, 520 Edgemont Road, Charlottesville, VA 22903, ³Planetary Science Institute, 1700 East Fort Lowell, Suite 106, Tucson, AZ 85719, ⁴NASA Goddard Space Flight Center, Astrochemistry Laboratory Code 691, 8800 Greenbelt Rd., Greenbelt, MD 20771,
⁵Department of Physics, American University, 4400 Massachusetts Ave NW, Washington, DC 20016.

Introduction: The analysis of terahertz and microwave (sub-millimeter/millimeter wavelengths, hereafter referred to as microwave) thermal emission from near-Earth asteroids can be used to constrain thermophysical (thermal inertia, emissivity) and radiative (index of refraction, loss tangent) properties of the top few centimeters of asteroid regolith. These properties can be used to constrain the regolith porosity. For near-Earth asteroids (NEAs), regolith porosity is one of the physical properties that should be known for the development of impact risk mitigation missions [1], as it has direct relevance to the mechanical properties of the material.

Regolith porosity and density gradients: The use of passive microwave observations, especially when combined with thermal infrared data, can be used to constrain regolith porosity and near surface vertical density gradients. This was demonstrated by the Microwave Instrument for the Rosetta Orbiter (MIRO) instrument [2], on board the Rosetta Spacecraft, when it made observations of two Main Belt Asteroids (MBAs): (2867) Šteins and (21) Lutetia. Combined observations of (21) Lutetia from MIRO and VIRTIS (near infrared spectrometer) determined the asteroid has a low thermal inertia surface, but that the thermal inertia increased with depth [3]. For daytime VIRTIS observations to be consistent with the MIRO nighttime thermal inertia, a surface roughness equivalent of 50% coverage of hemispherical craters was needed. Observations of (2867) Šteins suggest a thin layer of regolith [4] on top of a more rock-like layer [5]. This shows the importance of using multi-wavelength datasets to fully characterize both the horizontal and vertical variation of natural surfaces.

Methodology: Here we present a framework (Fig. 1) to determine asteroid regolith properties, based on [6], that combines thermal, radiative transfer, and regolith thermophysical models that can be compared to observed passive mm-wave thermal emission from ground observations. The thermal model used is KRC [7] (named after definition of thermal inertia $\sqrt{k\rho c}$), the radiative transfer model is that used by [6], and the regolith thermophysical model is based on [8]. This approach requires *a priori* knowledge of the object's composition, Bond albedo, shape, size, orbit, and spin properties. Comparisons of outputs from the series of models to observations provide best-fit estimates of thermal inertia, index of refraction, loss tangent, and effective emissivity. These best-fit solutions are then used to estimate surficial density, porosity, and effective grain size. This approach was originally developed assuming sufficient spatial resolution to observe temperatures at a range of latitudes and local times, thus allowing for the constraint of multiple parameters. However, most NEAs, even at close approach, are not spatially resolved by ground-based microwave telescopes. Therefore, our analysis will require surface parameters to be constrained from other observations. Fortunately, close approaches afford opportunity for a wide range of observations across the electromagnetic (EM) spectra that can constrain the regolith surface properties. Passive microwave thermal emissions at a range of frequencies, and therefore a range of penetration depths, can further constrain the regolith's near surface properties.

Ganymed as a case study multi-wavelength campaign: To demonstrate this multi-wavelength approach, observations of (1036) Ganymed have already been collected and are being analyzed (Table 2). Examples of observations are shown in Fig 2. Examples of modeled surface temperatures overlaid on a Database of Asteroid Models from Inversion Techniques (DAMIT) shape model is shown in Fig. 3.

Discussion: The next step in analysis is application of the radiative transfer code to determine expected observed flux, which can then be compared to observed flux. That comparison will determine a series of best-fit solutions for a suite of indices of refraction, loss tangents, thermal inertia, and effective surface emissivity. These properties will then be used to constrain density, porosity, and grain size. Because we have observations of multiple frequencies, we will be able to also constrain depth gradients for these regolith properties.



Acknowledgments & Disclaimers: This research program is supported through NASA ROSES Near-Earth Object Observations program grant 23-YORPD23_2-0034. Any use of trade, firm, or product names is for descriptive purposes only and does not imply endorsement by the U.S. Government. This content is preliminary and is subject to revision. It is being provided to meet the need for timely best science. The information is provided on condition that neither the U.S. Geological Survey or the U.S. Government shall be held liable for any damages resulting from the authorized or unauthorized use of this information.

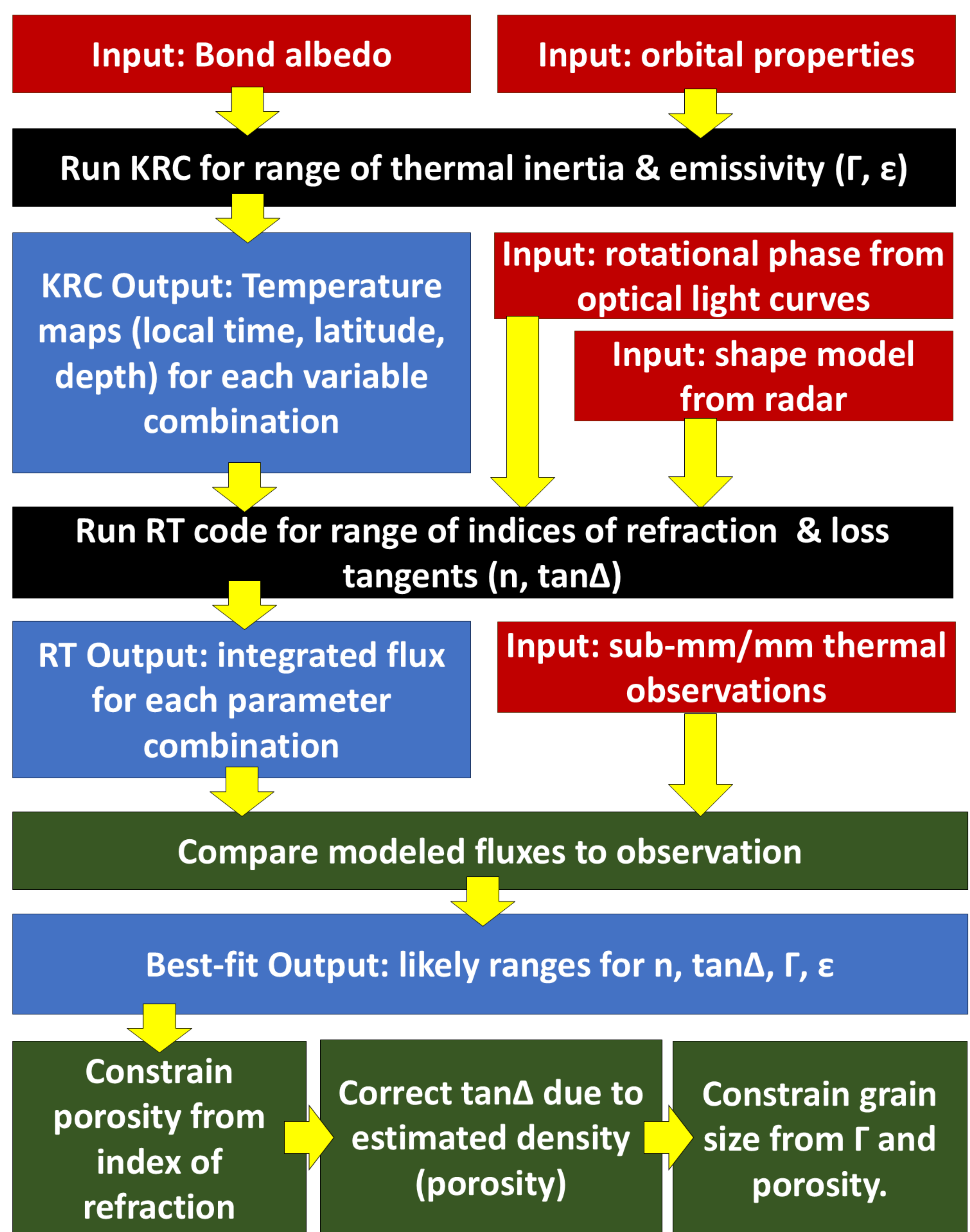


Figure 1: Flow chart of the methodology. Red indicates input parameters. Black indicates models. Blue indicates output. Green indicates analysis steps.

Table 1: A list of (1036) Ganymed observations acquired in Sep/Oct 2024.

Target	UT Date	UT Time	Telescope ^a	Wavelength
Ganymed	9/18/2024	18:10 - 18:35	IRAM	2.06 / 2.30 mm
	9/19/2024	15:10 - 17:13	IRAM	3.33 / 3.99 mm
	10/14/2024	04:00 - 12:25	SMA	1.3 mm
	10/16/2024	04:10 - 12:15	SMA	1.3 mm
	10/23/2024	04:34 - 07:59	VLA	30, 20, 9 mm
	10/23/2024	04:00 - 08:00	VLA	30, 20, 9 mm

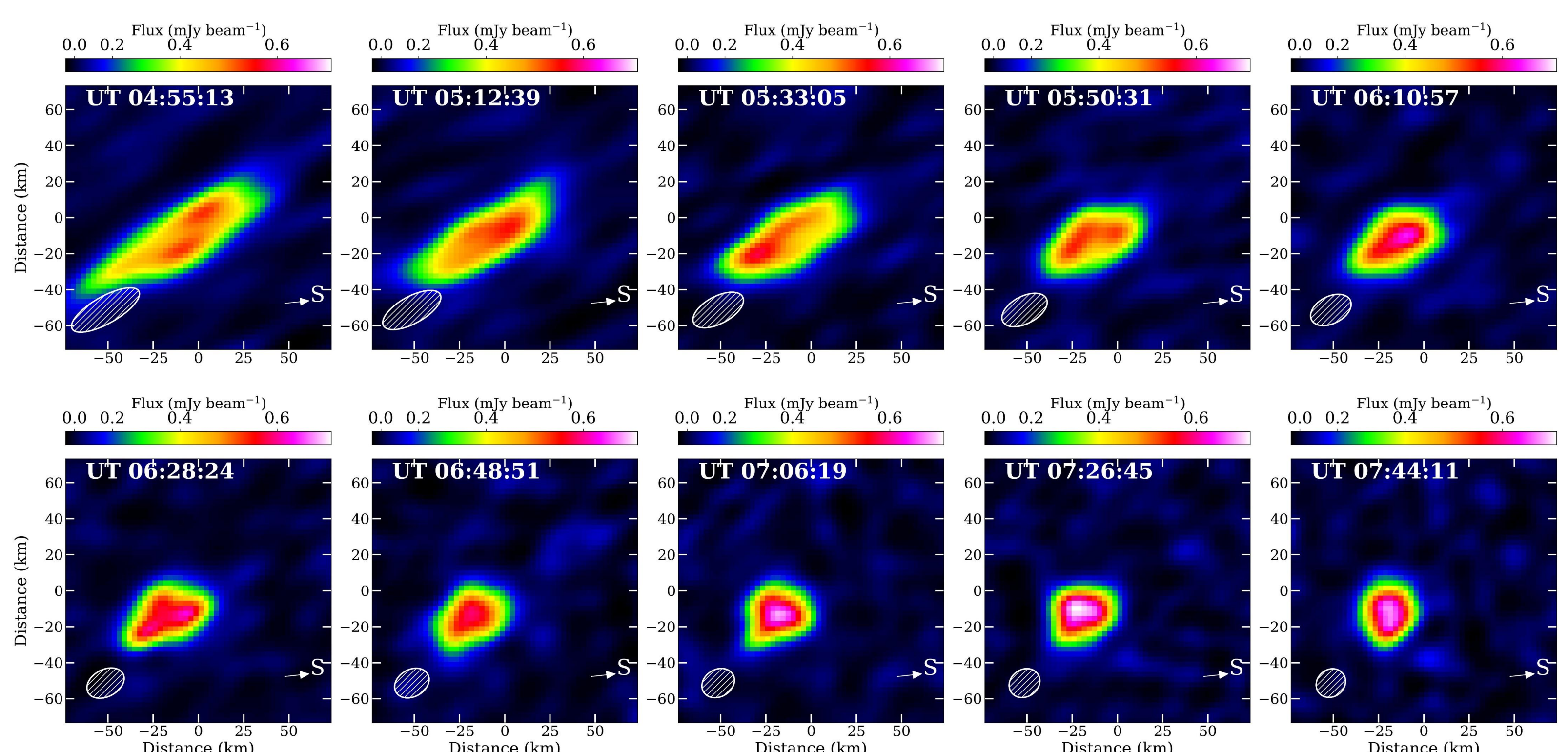


Figure 2: Examples of Ganymed Ka Band (9 mm wavelength) observation, 23 October 2024. The ellipses in the lower left of each frame is the beam size.

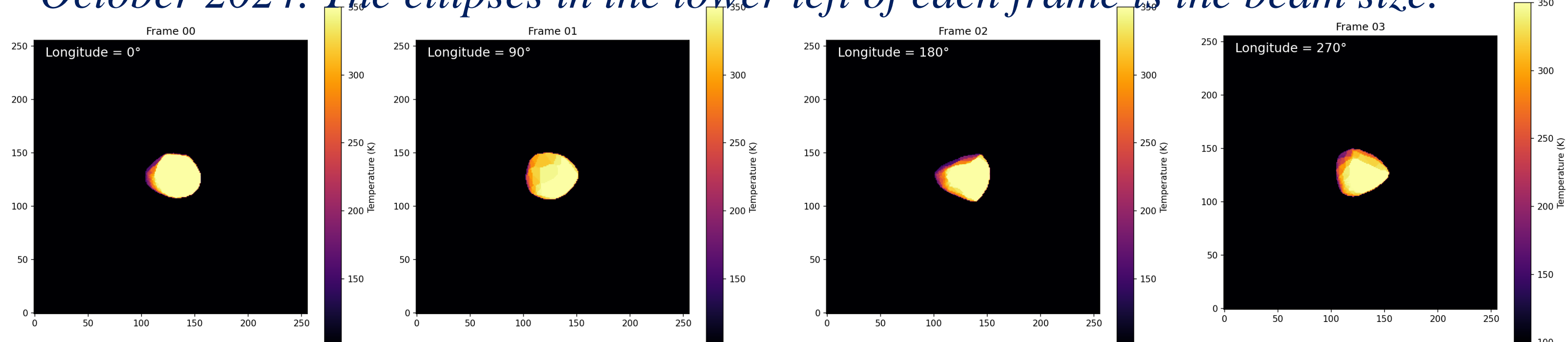


Figure 3: Examples of modeled surface temperature ($\Gamma=80$ tiu, $\epsilon=0.9$) overlaid on the Ganymed DAMIT shape model at four rotation phases; shape matters!

References: [1] Levasseur-Regourd A. et al. (2006), *Adv. in Space Res.*, 37(1), 161-168. [2] Gulikis S. et al. (2007) *SSR*, 128, 561-597. [3] Keihm S. et al. (2012) *Icarus*, 221(1), 395-404. [4] Leyrat C. et al. (2011) *A&A*, 531, id.A168. [5] Gulikis S. et al. (2010) *PSS*, 58(9), 1077-1087. [6] Li J-Y et al. (2020) *AJ*, 159(5), id.215. [7] Kieffer H. (2013) *JGR*, 118(3), 451-470. [8] MacLennan E. & Emery J. (2022) *PSJ*, 3(2), 47.